

Landscape genomic tests for associations between loci and environmental gradients

Eric Frichot¹ Sean Schoville¹ Guillaume Bouchard² Olivier François¹

(1) Université Joseph Fourier Grenoble, Centre National de la Recherche Scientifique, TIMC-IMAG

UMR 5525, 38042 Grenoble, France.

(2) Xerox Research Center Europe, F38240 Meylan, France.

Abstract

Adaptation to local environments often occurs through natural selection acting on a large number of alleles, each having a weak phenotypic effect. One way to detect these alleles is to identify genetic polymorphisms that exhibit high correlation with environmental variables used as proxies for ecological pressures. Here we propose an integrated framework based on population genetics, ecological modeling and statistical learning techniques to screen genomes for signatures of local adaptation. These new algorithms introduce latent factor mixed models to population genetics, employing an approach based on probabilistic principal component analysis in which population structure is introduced via unobserved variables. These fast, computationally efficient algorithms detect correlations between environmental and genetic variation while simultaneously inferring background levels of population structure. Comparing these new algorithms with related methods provides evidence that latent factor models can efficiently estimate random effects due to population history and isolation-by-distance patterns when computing gene-environment correlations, and decrease the number of false-positive associations in genome scans. We then apply these models to plant and human genetic data, identifying several genes with functions related to development that exhibit unusual correlations with climatic gradients.

1 Introduction

Local adaptation through natural selection plays a central role in shaping the variation of natural populations [1,2] and is of fundamental importance in evolutionary, conservation, and global-change biology [3–7]. The intensity of natural selection commonly varies in space, and can result in gene-environment interactions that have measurable effects on fitness (e.g. [8]). Adaptive divergence can then cause local populations to evolve traits that provide advantage under local environmental conditions.

In principle, identifying chromosomal regions involved in adaptive divergence can be achieved by scanning genome-wide patterns of DNA polymorphism [9,10]. Usually, the aim of screening procedures is to detect locus specific signatures of positive selection. In populations inhabiting spatially distinct environments, loci that underlie adaptive divergence can be detected by comparing relative levels of differentiation among large samples of unlinked markers [11,12] and by using empirical tests to compare levels of differentiation to the genomic background [13,14].

An alternative way to investigate signatures of local adaptation, especially when beneficial alleles have weak phenotypic effects, is by identifying polymorphisms that exhibit high correlation with environmental variables [3,15–18]. In natural populations, quantitative traits that exhibit continuous geographic variation are often associated with specific variables reflecting selective pressures acting on individual phenotypes [19]. This type of variation is then reflected in geographic clines or in sympatric populations that exploit different ecological niches [20]. Evidence for local adaptation to continuous environments can be detected if there is highly significant association with the environmental variables at some loci compared to the background genomic variation.

However the geographical basis of both environmental and genetic variation can confound interpretation of the tests [21], as local adaptation can be hindered by gene flow [22], and can be difficult to distinguish from the effects of genetic drift and demographic history [14]. As a consequence, when no corrections for the effects of population structure or isolation-by-distance are considered, tests for associations between loci and environmental variables using classical regression models are prone to high rates of false-positives [23]. Recent studies have used the background patterns of allele frequencies to build a null model which accounts for the effects of drift and demographic history [15,18,24,25]. To

correct for population stratification, [15] used an empirical approach that estimates the covariance of allele frequencies among populations. These authors assessed the evidence for local adaptation of each allele by testing whether or not environmental variables explained more variance than a null model with this particular covariance structure.

Here we argue that, unless a list of a priori selectively neutral loci are used to build the empirical covariance matrix, empirical tests may face a problem of circularity. The need to identify neutral loci from the genomic background before testing implies that these tests lack power to reject neutrality. In this study, we address this problem by introducing new statistical models, called latent factor mixed models. Using these models, we test correlations between environmental and genetic variation while estimating the effects of hidden factors that represent background residual levels of population structure. To perform parameter estimation, we extend probabilistic principal component analysis and recent statistical learning approaches [26–28]. Based on low rank approximation of the residual covariance matrix, we implement algorithms to deal with hundreds of thousands of polymorphisms with very rapid computing times. We show that our algorithms control for random effects due to population history and spatial autocorrelation when estimating gene-environment association, and we provide examples of how our approach can be used to detect local adaptation in plants and humans.

2 Method

Consider the data matrix, $(G_{i\ell})$, where each entry records the allele frequency in population or individual i at the genomic locus ℓ , $1 \leq i \leq n$, $1 \leq \ell \leq L$, and n and L represent the total sample size and number of loci, respectively. For simplicity, we assume our loci are biallelic, e.g. single nucleotide polymorphisms (SNPs), and data are available for each individual. In this case, for each marker, there is an ancestral and a derived allele, and $G_{i\ell}$ is the number of derived alleles for locus ℓ and individual i . For diploid data, $G_{i\ell}$ is thus equal to 0, 1 or 2, and corresponds to the genotype at locus ℓ . In addition to the genotypic data, we have a vector of d geographic and environmental variables, (X_i) , for each individual. The vector of covariates could include latitude and longitude, habitat and other ecological information, climatic variables, etc, that serve as proxies for unknown environmental pressures (For example, see [15, 21]).

Model. To evaluate associations between allele frequencies and environmental variables while correcting for background levels of population structure, we regard the matrix G as being a response variable in a regression mixed model

$$G_{i\ell} = \mu_\ell + \beta_\ell^T X_i + U_i^T V_\ell + \epsilon_{i\ell}, \quad (1)$$

where μ_ℓ is a locus specific effect, β_ℓ is a d -dimensional vector of regression coefficients, U_i and V_ℓ are scalar vectors with K dimensions ($1 \leq K \leq n$). The residuals $\epsilon_{i\ell}$ are statistically independent Gaussian variables of mean zero and variance σ^2 . We use Bayesian analysis to estimate the regression coefficients and their standard deviations. We assume Gaussian prior distributions on μ_ℓ and $\beta_{\ell j}$ with means equal to zero and variances σ_μ^2 and $\sigma_{\beta_j}^2$ ($\beta_{\ell j} \sim N(0, \sigma_{\beta_j}^2)$). Prior distributions on U_i and V_ℓ are Gaussian distributions with means equal to zero and constant variance for each component (the components are independent random variables). The variance of V_ℓ is set to $\sigma_V^2 = 1$, and all other prior distributions on variances are non-informative. We refer to the above statistical model as a *Latent Factor Mixed Model* (LFMM).

In LFMMs, environmental variables are introduced as fixed effects while population structure is modeled via latent factors. To separate neutral variation from adaptive variation, the matrix term $U^T V$ models the part of genetic variation that cannot be explained by the environmental pressures. Note that the use of factorization methods is closely related to estimating population structure via singular value decomposition, a well-established technique for identifying scores and loadings in principal component analysis (PCA, [29]). Recently, matrix factorization methods have been generalized to include probabilistic PCA [26] and probabilistic matrix factorization algorithms [27], which have proven useful in analyzing population genetic data [28]. To clarify the connection between LFMM and PCA, assume that no environmental variable is available. In this case, we set $\beta_\ell = 0$ for all locus ℓ . In matrix factorization algorithms, a data matrix G with n rows and L columns can be decomposed into a product of two matrices U and V , where U has n rows and K columns, and V is a K -by- L matrix. Following [30], we assume that the genotypic data are centered. We consider the matrix $Y_{i\ell} = G_{i\ell} - \bar{G}_{\cdot\ell}$, where we have subtracted the mean value of each column, $\bar{G}_{\cdot\ell} = \sum_{i=1}^n G_{i\ell}/n$. For

each individual i and locus ℓ , the decomposition is

$$Y_{i\ell} = U_i^T V_\ell = \sum_{k=1}^K U_{ik} V_{k\ell}. \quad (2)$$

To estimate the factor vectors U_i and V_ℓ , the squared error is minimized on the set of observed data

$$\min_{U,V} \sum_{k=1}^K (Y_{i\ell} - U_{ik} V_{k\ell})^2. \quad (3)$$

With $K = L$, this approach is similar to computing PCA loadings and scores [29]. The number of components K can, however, be chosen much lower than the number of loci or individuals. In simulations, we based our choice of K on Tracy-Widom theory [30]. In real applications, this choice of K may be replaced by other estimates of population genetic structure. When values are lower than 50, our algorithm is essentially a low-rank approximation of the covariance structure [31], which leads to computationally fast estimation algorithms.

To simultaneously estimate scores and loadings, environmental effects and biases, we implemented a Gibbs sampler algorithm for LFMMs (File S1). The Gibbs sampler is based on computing products of matrices of low dimension (typically, $K \leq 50$), and its speed scales with the current size of SNP data sets, around $n \approx 1,000$ and $L \approx 500,000$. In addition, we implemented a stochastic algorithm to compute standard deviations and $|z|$ -scores for the environmental effects. Using the empirical distribution of $|z|$ -scores obtained from all L loci, we compared each locus to the genomic background and retained loci with $|z|$ -scores exhibiting the highest absolute values. From a preliminary set of experiments using data simulated from the model defined in equation (1), we found that the estimates of fixed effects stabilized quickly, after 1,000 to 10,000 sweeps for $n = 100 - 1,000$ individuals and $L = 1,000 - 100,000$ loci. A 10-fold increase in the number of sweeps, however, was necessary to recover the true values of the latent factors. Additionally, we developed numerical optimization methods to compute *maximum a posteriori* (MAP) estimates for the LFMM. One of these methods, the alternate least square method uses deterministic steps that are similar to our stochastic Gibbs sampler [32]. When checking for convergence of the MCMC algorithm, we also found that least square estimates of regression coefficients were close to the point estimates computed by the Gibbs sampler method.

Theoretical considerations. Incorporating population genetic structure via estimates of admixture proportions or principal component analysis is common in genome-wide association studies [33, 34]).

[18] developed an alternative approach to identify loci underlying local adaptation in the computer program **Bayenv**. To explain the difference between our approach and **Bayenv**, suppose that we start by computing PCA scores from the matrix Y for all individuals, and denote by \tilde{U}_i the PCA scores for individual i . The product matrix $\tilde{U}\tilde{U}^T$ is thus equal to the empirical covariance matrix

$$\tilde{U}\tilde{U}^T = YY^T/n. \quad (4)$$

Now using the scores as covariates in a Bayesian regression model, we obtain

$$G = \mu + \beta^T X + \tilde{U}^T V + \epsilon. \quad (5)$$

By a change of variables, this is equivalent to fitting the model

$$G = \mu + \beta^T X + \tilde{\epsilon} \quad (6)$$

where the distribution of $\tilde{\epsilon}$ is a multivariate Gaussian distribution of the covariance matrix equal to $\sigma^2 \text{Id} + \sigma_V^2 YY^T/n$ (Id is the n -dimensional identity matrix). Setting $\sigma_V^2 = 1$ and considering small values of the scaling parameter σ^2 , the model defined in equation (6) is nearly equivalent to the model implemented in **Bayenv**. In a Bayesian Gaussian regression framework, incorporating PCA scores as covariates in an association model is equivalent to modeling residuals as Gaussian vectors with covariance depending on the empirical covariance matrix of the genotypic data. Though the **Bayenv** model uses a different link function, its residual term has the same covariance matrix as the genotypic data. From a theoretical point of view, the main difference between the **Bayenv** model and LFMM is the inference of the factor matrix U which is done in a fully Bayesian algorithm in LFMMs and in an empirical Bayes algorithm in **Bayenv** (see Discussion).

3 Simulation Study

We designed experiments based on simulated data to answer the following questions: 1) Are tests based on LFMMs conservative or liberal? 2) How does the LFMM algorithm perform compared to existing methods such as logistic or standard regression models [3], principal components regression and other existing mixed models [18]?

Distribution of P -values under the null hypothesis. We used equation (1) with $\beta = 0$ to generate data under a null hypothesis of no association with any environmental variables. In these experiments, we set the number of individuals to $n = 100$, and the number of loci to $L = 1,000$. We used 6 values, $K = 1, 3, 5, 7, 10$ and 20, for the rank of the factor matrix, V . For each series of experiments, we generated 10 replicates of this generative model, and we studied the distributions of P -values for tests using LFMMs. In these tests, we set the rank of the factor matrix equal to the values we used to generate simulations.

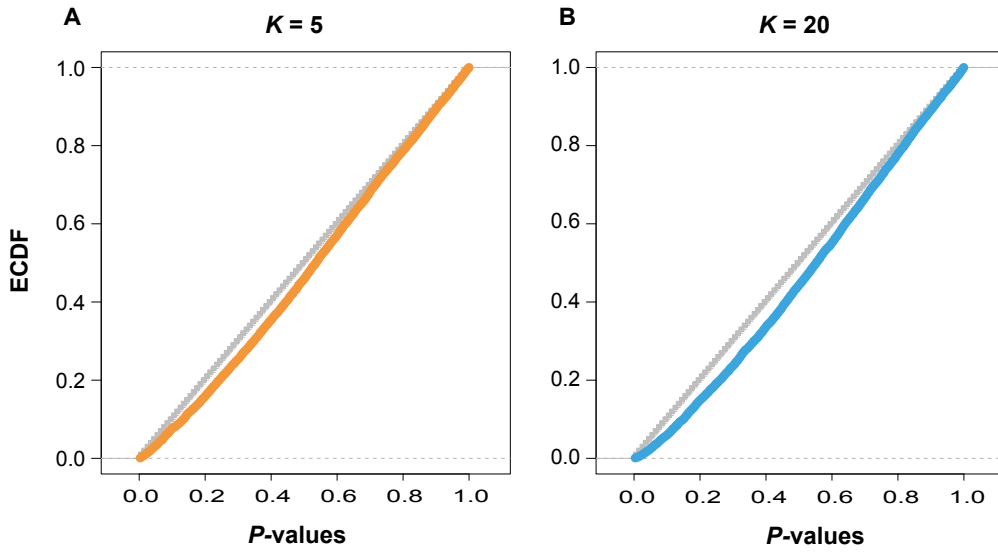


Figure 1: Empirical cumulative distribution function (ECDF) for LFMM tests for simulations from a generative model using A) $K=5$, B) $K=20$ latent factors.

Figure 1 reports the empirical cumulative distribution function (ecdf) for $K = 5$ and $K = 20$. Plots for the other values of K are shown in Figure S1. For values of K lower than 5, the ecdf was close to a uniform distribution. For $K = 20$, the tests were slightly conservative. Thus, for moderate and for large values of the number of latent factors, the tests produced small numbers of false positive associations.

Next we used equation (1) to generate data showing various levels of population structure and association with an environmental variable. The environmental variable was uniformly generated in the range $(0,1)$. Here we used 3 values for the rank of the factor matrix, $K = 2, 20$ and 100,

representing low, moderate and high levels of underlying population genetic structure. For each series of experiments, we generated 20 replicates of the generative model and compared the distribution of statistical errors for three estimation approaches: 1) LFMM, 2) standard linear regression model, 3) PC regression model. With the notations from section 2, these models were defined as follows. The LFMM was defined by equation

$$G_{i\ell} = \mu_\ell + \beta_\ell^T X_i + U_i^T V_\ell + \epsilon_{i\ell}$$

where we set the rank of the factor matrices equal to the values we used to generate simulations. The standard regression model was defined as

$$G_{i\ell} = \mu_\ell + \beta_\ell^T X_i + \epsilon_{i\ell} . \quad (7)$$

The PC regression model was defined as

$$G_{i\ell} = \mu_\ell + \beta_\ell^T X_i + \tilde{U}_i^T V_\ell + \epsilon_{i\ell} , \quad (8)$$

where (\tilde{U}_i) are the first K PCs computed from the matrix G . To compute point estimates of environmental effects and their $|z|$ -scores, Gibbs sampler algorithms were run for 1,000 sweeps after a burnin period of 100 sweeps. For these particular run length parameters, we checked that similar estimates were obtained for distinct initializations of the algorithm. For each locus, we recorded both the true, B_ℓ , and estimated environmental effects, \hat{B}_ℓ , and evaluated the absolute error

$$E_\ell = \left| \beta_\ell - \hat{\beta}_\ell \right| .$$

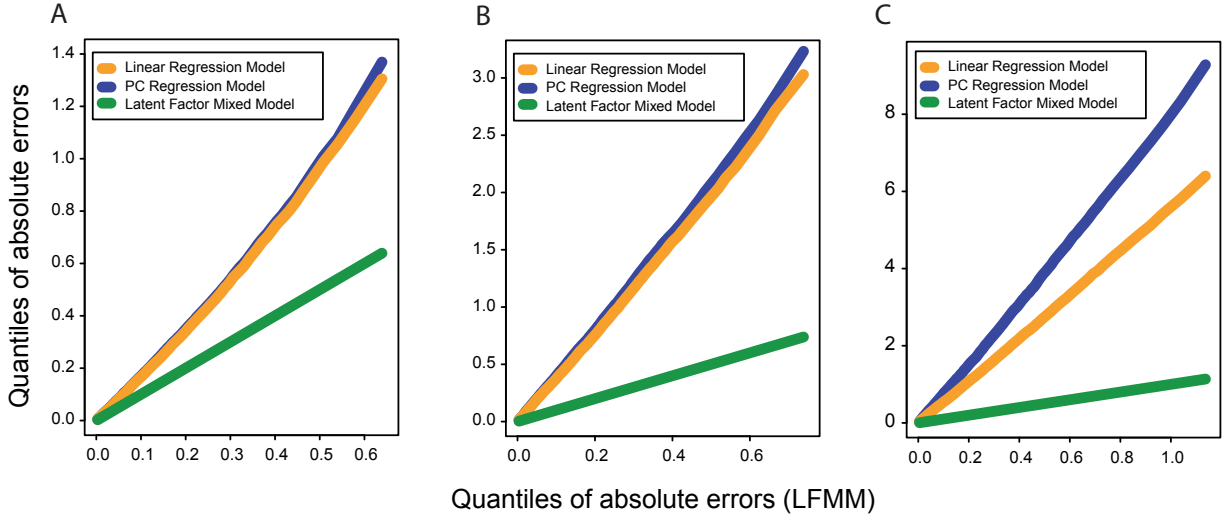


Figure 2: Quantiles of absolute errors for the standard linear regression, PC regression and LFM models using simulations from the LFM model with A) $K=2$, B) $K=20$ and C) $K=100$ latent factors.

Figure 2 reports the quantiles of absolute errors for the LFMM, the standard linear regression and PC regression models. For the LFMM, absolute errors ranged between 0 and 0.6 for $K = 2 - 20$, and between 0 and 1.0 for $K = 100$. Mean squared errors indicated that the bias and variance of estimates were small (Table 1). Compared to LFMMs, the relative errors of the linear and PC regression estimates increased with the rank of the hidden factor matrix. The absolute errors of these algorithms ranged between 0 and 1.4 for $K = 2$, between 0 and 3.2 for $K = 20$, and between 0 and 9.2 for $K = 100$. When linear or PC regression models were fitted to the data, the quantiles of errors shifted to values ≈ 1.74 -fold higher for $K = 2$, ≈ 3.8 to 4.1-fold higher for $K = 20$, and ≈ 5.5 to 7.7-fold higher for $K = 100$. Mean squared errors provide additional evidence of relatively poor performances of the linear regression and PC regression estimates when levels of underlying structure increase (Table 1).

Spatial coalescent simulations. In another series of experiments, we compared the LFMM estimation algorithm against two methods that do not correct for population stratification, and against two methods that use the empirical covariance matrix as a correction. The first set of methods include a linear model and generalized linear model (LM and GLM, [3]), and the second set of methods include a PC regression model (PCRM) and the mixed model *Bayenv* [18]. To enable comparisons, we

simulated genotypic data from spatial coalescent models with the computer program `ms` [35]. Ten data sets were generated according to a linear stepping-stone model with 40 demes, setting the effective migration rate between pairs of adjacent demes to the value $4Nm = 25$. Sampling 5 individuals in each deme, each data set included a total of $n = 200$ haploid individuals genotyped at $L = 1,000$ SNP loci. Using Tracy-Widom tests implemented in `SmartPCA`, we found that the number of principal components with P -values smaller than 0.01 was around $K_{TW} = 7$. We ran the Gibbs sampler algorithm during 100 sweeps for burnin, and we used the next 900 sweeps to compute points estimates, variances and $|z|$ -scores.

Distribution of P -values. To examine the outcome of tests when genetic variation is neutral at all loci, we computed the distributions of P -values under a LM, GLM, PCRM and LFMM with different values for the number of latent factors (K ranging from 1 to 20). The distributions of P -values for tests based on LM and GLM showed a strong departure from the uniform distribution (Figure 3A-B). In those cases, the tests were too liberal, and produced a large number of false positive results. Using $K = 7$ latent factors or PCs, the distribution of P -values for tests based on an LFMM or PCRM was much closer to a uniform distribution (Figure 3C-D). In addition, we found that choosing K based on Tracy-Widom theory led to slightly conservative tests for the particular simulation settings used here. Ecdf for all values of K are shown in Figures S2 and S3, respectively.

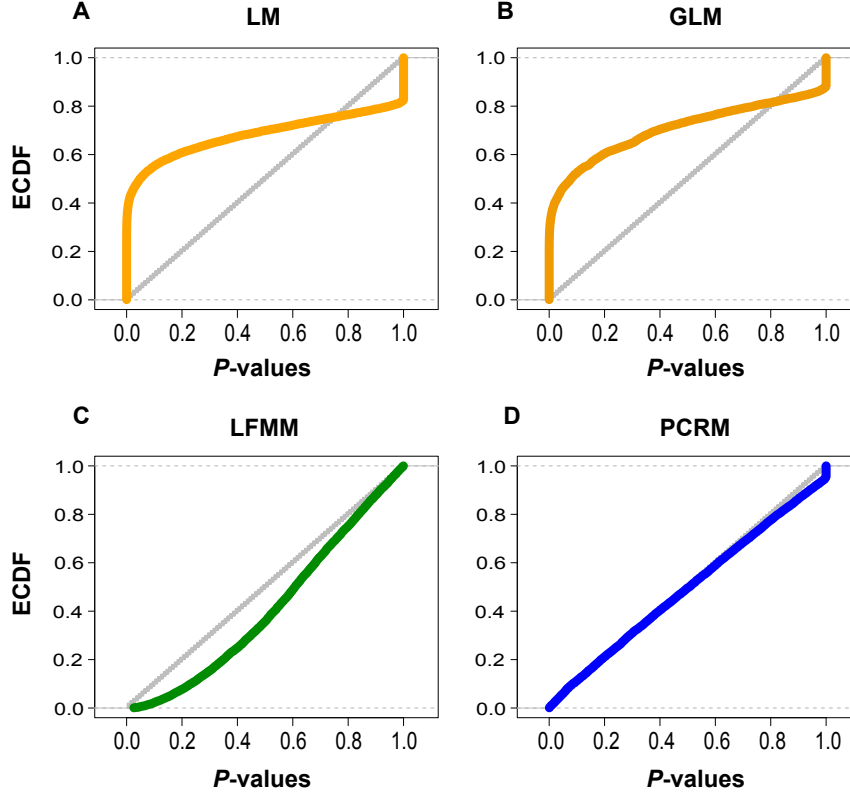


Figure 3: Empirical cumulative distribution function (ECDF) for A) the linear regression model (LM), B) the generalized linear model (GLM), C) the LFM model using $K = 7$ latent factors (LFMM), and D) the PC regression model using $K = 7$ principal components (PCRM).

Next we evaluated the ability of LFMMs to detect loci exhibiting correlations with particular environmental gradients, and compared tests based on an LFMM with methods based on linear models and the computer program `Bayenv` [18]. An environmental variable, x , was defined for each population as the geographic identifier of the population in the linear stepping-stone model. We created an environmental gradient using a logistic function, $s(x)$, of x as follows

$$s(x) = \frac{1}{1 + e^{\theta(x-20)}}, \quad \theta > 0. \quad (9)$$

For each of the 10 previously generated neutral stepping-stone simulations, we simulated binary alleles for each deme x at 50 loci with frequency $s(x)$, with the slope of the gradient $\theta = 0.2$. We then obtained 10 data sets with $L = 1050$ loci including 50 loci correlated with the environmental gradient, $s(x)$. Across these datasets, `smartPCA` estimates between 5 and 7 significant eigenvectors ($P < 0.01$ in the

Tracy-Widom test). For the simulated data sets, we evaluated the percentage of false negative (FN) and of false positive (FP) tests based on LM, GLM, PCRM and LFMM, for two values of the type I error (Table 2).

Using $\theta = 0.2$ in simulations of non-neutral loci, we found that linear models exhibited high percentages of FP. In contrast, tests based on PCRM exhibited very large percentages of FN, and had no power to reject neutrality. Tests based on LFMM produced low numbers of FP, and had reasonable power to reject the null hypothesis of no association.

Comparisons with Bayenv. For each of the 10 previously generated neutral stepping-stone simulations, we simulated binary alleles for each deme x at 50 loci with frequency $s(x)$, using $\theta = 0.1$. To enable comparison with the program **Bayenv**, which returns Bayes factors instead of P -values, we considered ranked lists recording the M loci corresponding to the strongest (true) associations (M between 1 and 1,050). For each M , we computed the number of true positives and the number of false negatives. Locus ranking was performed on the basis of $|z|$ -scores in LFMM, and on the basis of Bayes factors in **Bayenv**. The LFMM tests used values of K equal to $K = 1, 3, 5, 7, 10$ and 20, and we used the default parameters of the **Bayenv** algorithm to compute Bayes factors (run length of 30,000 sweeps). Experiments were assessed by measuring the area under the receiver-operating characteristic curve (AUC) averaged over 10 replicates. The mean AUC for tests based on LFMM with $K = 5 - 7$ factors were around 0.95 – 0.96 whereas the AUC for **Bayenv** was equal to 0.88. In the linear stepping stone model simulations, the tests based on LFMM obtained better performances than **Bayenv** for all values of K (Figure 4).

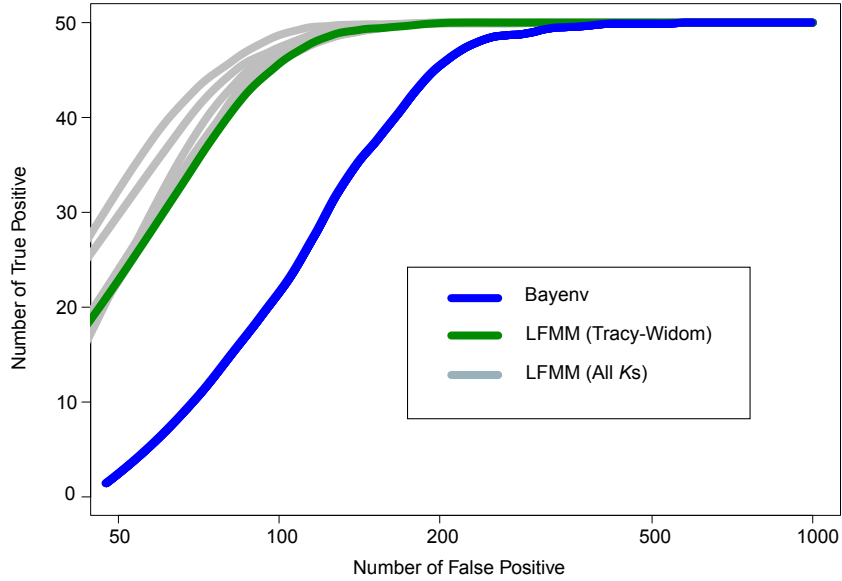


Figure 4: Detection of outlier loci. Number of true positives for the **Bayenv** model and the Latent Factor Mixed Model for $K = 7$ (Tracy-Widom value) and for $K = 1, 3, 5, 10, 20$ for spatial coalescent simulations including loci under selection.

4 Data Analysis

To illustrate the application of LFMMs, we analyzed genomic data sets of Loblolly Pines (*Pinus taeda*, Pinaceae, [21]) and humans (Human Genome Diversity Panel, [36]).

Loblolly Pine

The Loblolly Pine is distributed throughout the southeastern USA, ranging from the arid Great Plains to the humid Eastern Temperate Forest ecoregion. The data consisted of 1,730 SNPs selected in expressed sequence tags (EST) for 682 individuals [21]. Following [21], we considered 5 environmental variables representing the five first components of a PCA for 60 climatic variables. The first component (PC1) was mainly described by latitude, longitude, temperature and winter aridity. PC2 was described by longitude, spring-fall aridity and precipitation [21].

For each of the 5 environmental variables, we applied the LFMM algorithm using 100 sweeps for burnin and 400 additional sweeps to compute $|z|$ -scores for all loci. Based on a prior analysis of the genotypic data with the program **SmartPCA**, we used $K = 10$ latent factors. A total of 392,

113 and 30 SNPs obtained $|z|$ -scores greater than 3, 4 or 5 for at least one environmental variable, respectively. Based on this result, we considered that a SNP effect was significant when its $|z|$ -score was greater than 4 (two-sided test). Among the 50 loci with the highest $|z|$ -scores, 17 were shared with those detected by [21] using **Bayenv**. Seven of the 10 SNPs with Bayes factors greater than 10^3 were confirmed by the LFMM analysis. For the first and second environmental variables, the two SNPs which obtained the highest Bayes factors using **Bayenv** were recovered by the LFMM analysis. Table 3 provides a list of SNPs associated with climatic gradients and their functional annotation. Compared to the analysis of [21], the LFMM analysis discovered new significant and interesting associations with climatic gradients, for example, the chloroplast lumen 19 kDA protein involved in photosynthesis ($|z| = 6.42$), a pentatricopeptide repeat protein involved in oxidative stress and salt stress ($|z| = 5.90$), and the heat shock transcription factor hsf5 ($|z| = 5.60$) involved in regulation of transcription and response to temperature stress (Table 3 and Table S1).

Human data analysis

We applied an LFMM analysis to a worldwide sample of genomic DNA from 1,043 individuals in 52 populations, referred to as the Human Genome Diversity Project – Centre Etude Polymorphisme Humain (HGDP-CEPH) Human Genome Diversity Cell Line Panel (hagsc.org/hgdp/). The genotypes were generated on Illumina 650K arrays [36], and the data were filtered to remove low quality SNPs included in the original files.

We extracted climatic data for each of the 52 population samples using the WorldClim data set at 30 arcsecond (1km^2) resolution [37]. These data include 11 bioclimatic variables interpolated from global weather station data collected during a 50 year period (1950-2000). The climatic variables included annual mean temperature, mean diurnal range, maximum temperature of warmest month, minimum temperature of coldest month, annual precipitation, etc (Table S2). We summarized the climatic variables by using the first axis of a principal component analysis. For this first principal component, we applied the LFMM algorithm to compute $|z|$ -scores for each locus with $K = 50$ latent factors, using 100 sweeps for burnin and 900 additional sweeps to warrant convergence.

A total of 2,624 (0.4%), 508 (0.08%) and 65 (0.007%) SNPs obtained $|z|$ -scores greater than 5, 6 or 7, respectively (Figure S3). Among loci with $|z|$ -scores greater than 5, 28 GWAS-SNPs with known

disease or trait association were found [38]). These include several SNPs discovered by [24]. For example the SNPs rs12913832 and rs28777, $|z|$ -scores greater than 6, are associated with genes OCA2 and SLC45A2 (Table 4). Among the SNPs significantly correlated with climatic gradients, several notable examples include genes associated with celiac disease (ICOSLG), height (LHX3-QSOX2 and IGF1), and vitamin D synthesis or activation (NADSYN1 encoding nicotinamide adenine dinucleotide synthetase and DHCR7 the gene encoding 7-dehydrocholesterol reductase, an enzyme catalyzing the production in skin of cholesterol from 7-dehydrocholesterol (Table 4). Among the 65 SNPs with $|z|$ -scores greater than 7, 31 were located within genes (Table S3). One interesting result is that several genes are associated with multicellular organismal development. EPHB4 ($|z| = 8.90$) is involved in heart morphogenesis and angiogenesis, NRG1 ($|z| = 7.15$) involved with nervous system development and cell proliferation, RBM19 ($|z| = 7.04$) involved with positive regulation of embryonic development, EYA2 ($|z| = 7.09$) involved with eye development and DNA repair, and POLA1 ($|z| = 7.63$) involved with the mitotic cell cycle and cell proliferation [39, 40].

5 Discussion

Interpretation of LFMM results and other methods. Based on a matrix factorization approach, LFMMs incorporate a unified framework for estimating effects of environmental and demographic factors on genetic variation. Without environmental variables, LFMMs are equivalent to performing a probabilistic PCA of allele frequencies [26]. When environmental variables are included, hidden factors capture the part of genetic variation that cannot be explained by the set of measured environmental variables. This fraction of genetic variation could result from the demographic history of the species, unknown environmental pressures or from IBD patterns.

While a plethora of statistical tests have been proposed for detecting genes evolving under positive selection and local adaptation [10, 14], the development of tests based on correlations with habitat or landscape variables is still recent [3, 15]. Compared to methods based on summary statistics, tests based on environmental association have increased power to detect selection from standing genetic variation and soft sweeps in a species genome [6, 17]. However, simple implementation of these tests, for example simple linear or logistic regression models, can be misleading in the presence of IBD

patterns [23]. Our simulation results provide clear evidence that tests based on LFMMs significantly reduce the rates of false positive associations in the presence of IBD.

While both the mixed model approach of the computer program **Bayenv** and the LFMM approach includes a covariance structure in a regression model, there are important differences between the two approaches. A first improvement is that LFMMs estimate latent factors and regression coefficients simultaneously, while **Bayenv** first estimates a covariance matrix, and then uses it when estimating (random) environmental effects. To apply **Bayenv**, the authors suggest utilizing selectively neutral SNPs to estimate the covariance matrix. This approach requires separating neutral from adaptive variation a priori, and is difficult to apply when selection acts on phenotype at a large number of loci. Inclusion of adaptive markers in the "neutral set" is sometimes unavoidable, and in this case, **Bayenv** may overlook interesting associations. This distinction between approaches explains the observed differences in the lists of outlier loci for Loblolly pines, where 1,730 SNPs were genotyped in expressed sequences. For these data it was extremely difficult to select neutral SNPs from the background a priori. Another distinction between LFM and **Bayenv** approaches is our use of low rank approximations of the covariance matrix. LFMMs actually estimate correlations between environmental predictors and allele frequencies while K hidden factors explain residual genetic variation, where K is much smaller than the sample size. The low rank approximation is computationally faster than **Bayenv** when analyzing large data sets.

Number of latent factors. In the LFM modeling approach, the choice of low values for K is important for optimizing the computational performances of the estimation algorithm. This choice is reminiscent of selecting the number of components in PCA or in Bayesian clustering programs, and it has also an impact on test outcomes. For values of K taken too large, the tests are highly conservative, and the power to reject neutrality declines. Values of K that minimize the trade-off between the bias and variance for our statistical estimates could be obtained by using cross-validation procedures, but cross-validation procedures are computationally intensive, so instead we use Tracy-Widom theory to select K [30]. We evaluated this choice during our simulation analysis, and found that it led to slightly conservative tests. Although the choice of Tracy-Widom estimates is suboptimal, the performances of LFMMs were still superior to those of **Bayenv** in simulations of IBD patterns. In the analysis of

human data, we restricted K to be less than 50 (approximately the number of population samples). We suggest that, when there is a reasonable estimate of the number of genetic cluster for a species, it can be used in LFMM tests directly. While finer grain population structure could be evaluated [41], our choice was again motivated by a trade-off between accuracy and run-time. A future development of our LFMM approach will be to develop fast numerical optimization procedures based on variational approximations of the likelihood, which will allow us to implement cross-validation algorithms and increase the power of tests.

Plant and human data. For *Pinus taeda*, the LFMM results confirmed that several ESTs previously discovered with **Bayenv** had functions linked to climate [21]. In addition, the LFMM analysis discovered new interesting candidate SNPs. Those variants include functions associated with wound repair and immunity, photosynthetic activity and carotenoid biosynthesis, cellular respiration and carbohydrate metabolism, heat, salt and oxidative stress responses (Table 3). Applying LFMMs to the HGDP data, we found that a total of 0.4% of all polymorphisms (2,624 SNPs) exhibited significant associations with temperature gradients ($|z| > 5$). For example, we identified SNPs associated with the gene *OCA2* that may be functionally linked to blue or brown eye color and the gene *SLC45A2* that may be associated with skin pigmentation [24]. This list also contained SNPs associated with height and vitamin D synthesis and diseases such as gluten intolerance and Crohn’s disease. Our list of genic SNPs with $|z|$ -scores greater than 7 ($|z| > 7$) was enriched in genes involved in organismal development. For example, the genes *EPHB4*, *BOK*, and *NRG1* –with functions related to heart and brain development– were associated with climatic gradients. Overall, the analysis confirmed that many loci are associated with climatic gradients or to correlated evolutionary pressures (for example, pathogenic environment). This result supports the hypothesis that soft sweeps may have been common in recent human evolution [17].

Conclusion. With ever increasing amounts of genetic data generated by high-throughput sequencing technologies, population genetic methods have shifted from traditional statistical approaches to approaches that use statistical learning techniques. Estimates of ancestry and other population parameters are commonly obtained from mixture models [42–44], principal component analyses [30], hidden

Markov models [45] and factor analysis [28]. Our study contributes to the machine learning toolbox for population and landscape genomic analysis by implementing new gene-environment association tests based on matrix factorization methods.

Software availability. Source codes and computer programs for fitting LFMMs are available from the authors web-sites.

Acknowledgments. This work was supported by a grant from la Région Rhône-Alpes to Eric Fritchot and Olivier François, and by an NSF grant to Sean Schoville (OISE-0965038). Olivier François acknowledges support from Grenoble INP.

References

- [1] C Darwin. *On the Origin of Species by Means of Natural Selection, or the Preservation of Favoured Races in the Struggle for Life*. John Murray, 1859.
- [2] G C Williams. *Adaptation and Natural Selection*, volume 1996. Princeton University Press, 1966.
- [3] S Joost, A Bonin, M W Bruford, L Després, C Conord, G Erhardt, and P Taberlet. A spatial analysis method (SAM) to detect candidate loci for selection: Towards a landscape genomics approach to adaptation. *Molecular Ecology*, 16(18):3955–3969, 2007.
- [4] S Manel, S Joost, B K Epperson, R Holderegger, A Storfer, M S Rosenberg, K T Scribner, A Bonin, and M-J Fortin. Perspectives on the use of landscape genetics to detect genetic adaptive variation in the field. *Molecular Ecology*, 19(17):3760–3772, 2010.
- [5] R D Barrett and H E Hoekstra. Molecular spandrels: tests of adaptation at the genetic level. *Nature Reviews Genetics*, 12(11):767–780, 2011.
- [6] S D Schoville, A Bonin, O François, S Lobreaux, C Melodelima, and S Manel. Adaptive genetic variation on the landscape: Methods and cases. *Annual Review of Ecology, Evolution and Systematics*, in press 2012.

- [7] F Jay, S Manel, N Alvarez, E Y Durand, W Thuiller, R Holderegger, P Taberlet, and O François. Forecasting changes in population genetic structure of alpine plants in response to global warming. *Mol Ecol*, 21(10):2354–68, 2012.
- [8] J F Storz and C W Wheat. Integrating evolutionary and functional approaches to infer adaptation at specific loci. *Evolution*, 64(9):2489–2509, 2010.
- [9] R Nielsen. Molecular signatures of natural selection. *Annual Review of Genetics*, 39(1):197–218, 2005.
- [10] J F Storz. Using genome scans of DNA polymorphism to infer adaptive population divergence. *Molecular Ecology*, 14(3):671–688, 2005.
- [11] M A Beaumont and R A Nichols. Evaluating loci for use in the genetic analysis of population structure. *Proceedings of the Royal Society B Biological Sciences*, 263(1377):1619–1626, 1996.
- [12] M A Beaumont and D J Balding. Identifying adaptive genetic divergence among populations from genome scans. *Molecular Ecology*, 13(4):969–980, 2004.
- [13] J M Akey. Constructing genomic maps of positive selection in humans: where do we go from here? *Genome Research*, 19(5):711–722, 2009.
- [14] J Novembre and A Di Rienzo. Spatial patterns of variation due to natural selection in humans. *Nature Reviews Genetics*, 10(11):745–755, 2009.
- [15] A M Hancock, D B Witonsky, A S Gordon, G Eshel, J K Pritchard, G Coop, and A Di Rienzo. Adaptations to climate in candidate genes for common metabolic disorders. *PLoS Genetics*, 4(2):13, 2008.
- [16] B N Poncet, D Herrman, F Gugerli, P Taberlet, R Holderegger, L Gielly, D Rioux, W Thuiller, S Aubert, and S Manel. Tracking genes of ecological relevance using a genome scan in two independent regional population samples of *Arabis alpina*. *Molecular ecology*, 19(14):2896–2907, 2010.

- [17] J K Pritchard, J K Pickrell, and G Coop. The genetics of human adaptation: hard sweeps, soft sweeps, and polygenic adaptation. *Current Biology*, 20(4):R208–R215, 2010.
- [18] G Coop, D Witonsky, A Di Rienzo, and J K Pritchard. Using environmental correlations to identify loci underlying local adaptation. *Genetics*, 185(4):1411–1423, 2010.
- [19] J A Endler. *Geographic variation, speciation, and clines*. Princeton University Press, 1977.
- [20] J B S Haldane. The theory of a cline. *Journal of Genetics*, 48(3):277–284, 1948.
- [21] A J Eckert, A D Bower, S C González-Martínez, J L Wegrzyn, G Coop, and D B Neale. Back to nature: Ecological genomics of loblolly pine (*Pinus taeda*, pinaceae). *Molecular Ecology*, 19(17):3789–3805, 2010.
- [22] T Lenormand. Gene flow and the limits to natural selection. *Trends in Ecology & Evolution*, 17(4):183–189, 2002.
- [23] P G Meirmans. The trouble with isolation by distance. *Molecular Ecology*, 21(12):2839–46, 2012.
- [24] A M Hancock, D B Witonsky, G Alkorta-Aranburu, C M Beall, A Gebremedhin, R Sukernik, G Utermann, J K Pritchard, G Coop, and A Di Rienzo. Adaptations to climate-mediated selective pressures in humans. *PLoS Genetics*, 7(4):16, 2011.
- [25] M Fumagalli, M Sironi, U Pozzoli, A Ferrer-Admettla, L Pattini, and R Nielsen. Signatures of environmental genetic adaptation pinpoint pathogens as the main selective pressure through human evolution. *PLoS Genetics*, 7(11):e1002355, 2011.
- [26] M E Tipping and C M Bishop. Probabilistic principal component analysis. *BMC Bioinformatics*, 61(3):611–622, 1999.
- [27] R Salakhutdinov and A Mnih. Bayesian probabilistic matrix factorization using Markov chain Monte Carlo. *Proceedings of the 25th International Conference on Machine Learning (2008)*, 25(6):880–887, 2008.
- [28] B E Engelhardt and M Stephens. Analysis of population structure: A unifying framework and novel methods based on sparse factor analysis. *PLoS Genetics*, 6(9):12, 2010.

- [29] I T Jolliffe. *Principal Component Analysis*. Springer Verlag New York, 1986.
- [30] N Patterson, A L Price, and D Reich. Population structure and eigenanalysis. *PLoS Genetics*, 2:20, 2006.
- [31] C Eckart and G Young. The approximation of one matrix by another of lower rank. *Psychometrika*, 1(3):211–218, 1936.
- [32] R M Bell and Y Koren. Scalable collaborative filtering with jointly derived neighborhood interpolation weights. *Seventh IEEE International Conference on Data Mining ICDM 2007*, 07(1):43–52, 2007.
- [33] Alkes L Price, Nick J Patterson, Robert M Plenge, Michael E Weinblatt, Nancy A Shadick, and David Reich. Principal components analysis corrects for stratification in genome-wide association studies. *Nature Genetics*, 38(8):904–909, 2006.
- [34] J Yu, G Pressoir, W H Briggs, I Vroh Bi, M Yamasaki, J F Doebley, M D McMullen, B S Gaut, D M Nielsen, J B Holland, S Kresovich, and E S Buckler. A unified mixed-model method for association mapping that accounts for multiple levels of relatedness. *Nature Genetics*, 38(2):203–208, 2006.
- [35] R R Hudson. Generating samples under a wright-fisher neutral model of genetic variation. *Bioinformatics*, 18(2):337–338, 2002.
- [36] J Z Li, D M Absher, H Tang, A M Southwick, A M Casto, S Ramachandran, H M Cann, G S Barsh, M Feldman, L L Cavalli-Sforza, and Feldman M. Worldwide human relationships inferred from genome-wide patterns of variation. *Science*, 319(5866):1100–1104, 2008.
- [37] R J Hijmans, S E Cameron, J L Parra, P G Jones, and A Jarvis. Very high resolution interpolated climate surfaces for global land areas. *International Journal of Climatology*, 25(15):1965–1978, 2005.
- [38] L A Hindorff, P Sethupathy, H A Junkins, E M Ramos, J P Mehta, F S Collins, and T A Manolio. Potential etiologic and functional implications of genome-wide association loci for human diseases

and traits. *Proceedings of the National Academy of Sciences of the United States of America*, 106(23):9362–9367, 2009.

- [39] S F Saccone, J Quan, G Mehta, R Bolze, P Thomas, E Deelman, J A Tischfield, and J P Rice. New tools and methods for direct programmatic access to the dbSNP relational database. *Nucleic Acids Research*, 39(Database issue):D901–D907, 2011.
- [40] P V Hornbeck, J M Kornhauser, S Tkachev, B Zhang, E Skrzypek, B Murray, V Latham, and M Sullivan. Phosphositeplus: a comprehensive resource for investigating the structure and function of experimentally determined post-translational modifications in man and mouse. *Nucleic Acids Research*, 40(D1):D261–D270, 2012.
- [41] D J Lawson, G Hellenthal, S Myers, and D Falush. Inference of population structure using dense haplotype data. *PLoS Genetics*, 8(1):e1002453, 2012.
- [42] J K Pritchard, M Stephens, and P Donnelly. Inference of population structure using multilocus genotype data. *Genetics*, 155(2):945–959, 2000.
- [43] E Durand, F Jay, O E Gaggiotti, and O François. Spatial inference of admixture proportions and secondary contact zones. *Molecular Biology and Evolution*, 26(9):1963–1973, 2009.
- [44] D H Alexander and K Lange. Enhancements to the admixture algorithm for individual ancestry estimation. *BMC Bioinformatics*, 12(1):246, 2011.
- [45] A L Price, A Tandon, N Patterson, K C Barnes, N Rafaels, I Ruczinski, T H Beaty, R Mathias, D Reich, and S Myers. Sensitive detection of chromosomal segments of distinct ancestry in admixed populations. *PLoS Genetics*, 5(6):e1000519, 2009.

Supplementary Text 2

FIGURE S1: Empirical cumulative distribution function for LFMM tests for simulations from generative models with $K = 1, 3, 5, 10$, and 20 latent factors.

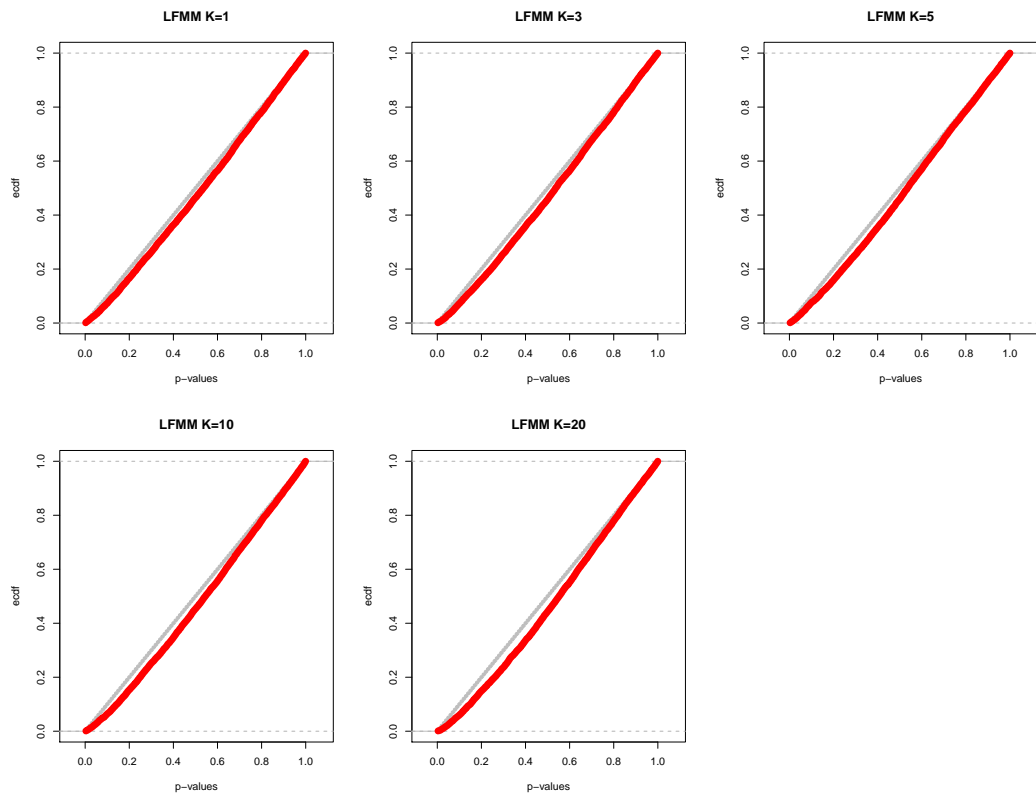


FIGURE S2: Empirical cumulative distribution function for the LFMM using $K = 1, 3, 5, 7, 10$, and 20 latent factors.

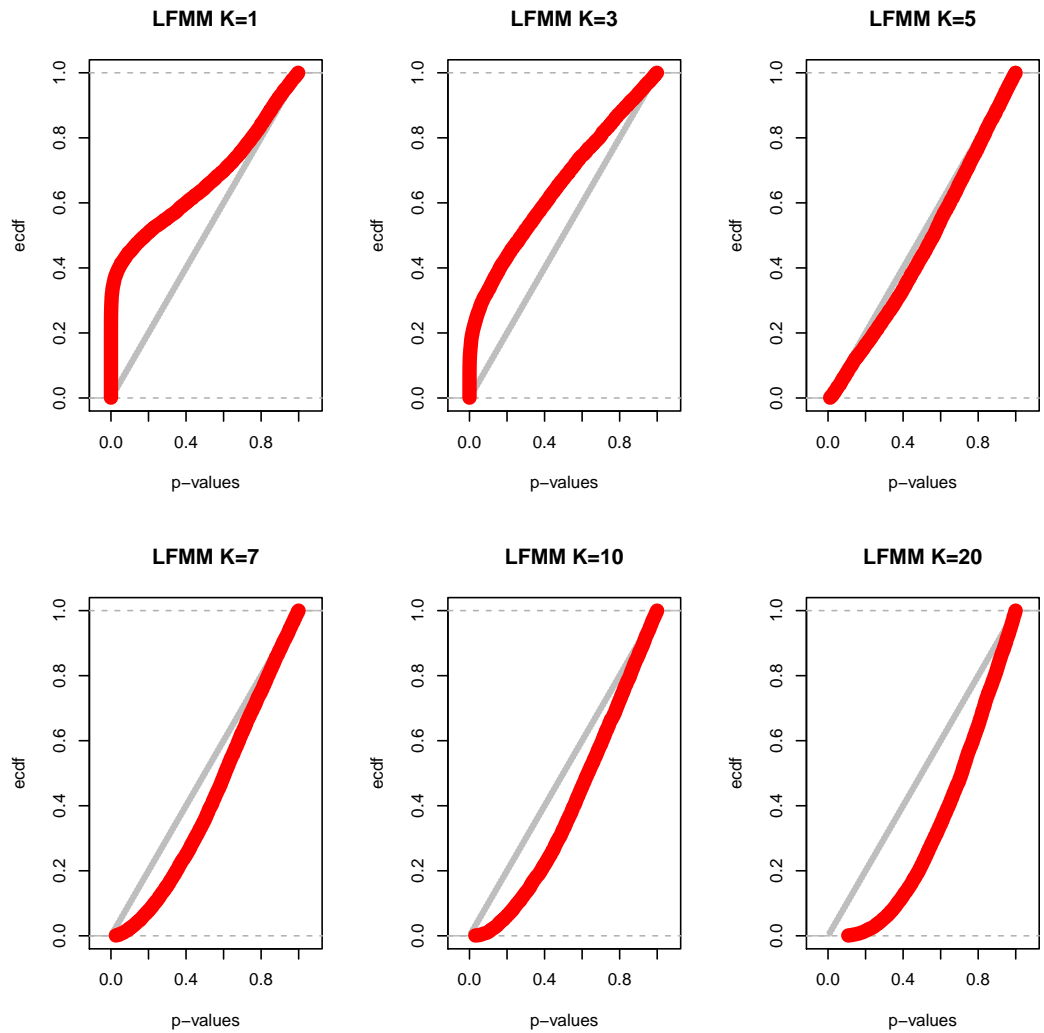
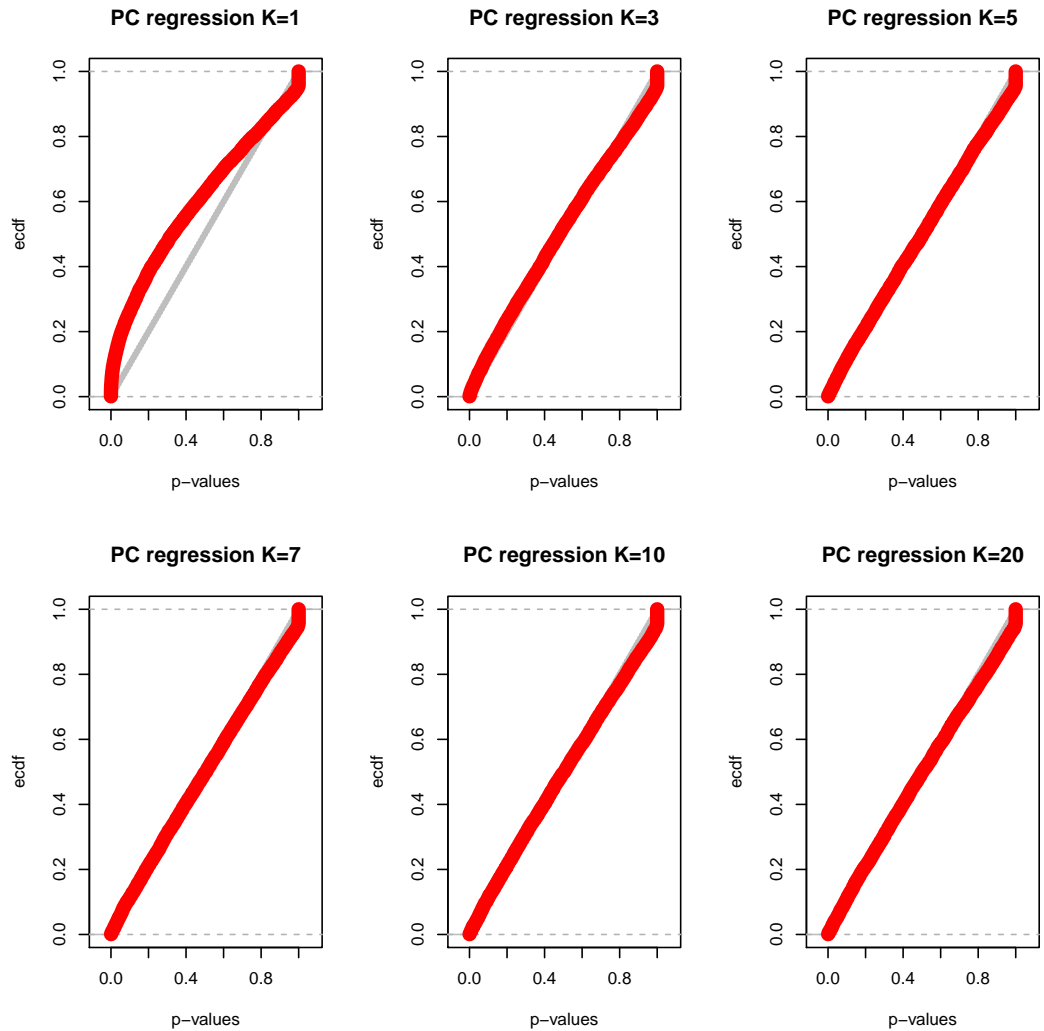


FIGURE S3: Empirical cumulative distribution function for the PC regression model using $K = 1, 3, 5, 7, 10,$ and 20 latent factors.



Tables

TABLE 1: Mean squared errors for estimates of environmental effects.

K	LM	PCRM	LFMM
2	0.20	0.21	0.15
20	1.27	1.42	0.08
100	6.13	12.41	0.20

TABLE 2: Percentage of false negative, FN and false positive (FP) for linear, PCR and LFM models and type I error α .

FN (FP)	LM	GLM	PCRM	LFMM
type I error:				
$-\log_{10} \alpha = 3$	0% (33%)	0% (24%)	100 % (3%)	4% (5%)
$-\log_{10} \alpha = 4$	0% (27%)	0% (19%)	100 % (0%)	14% (3%)

TABLE 3: Loblolly Pines. Annotation and gene ontology for some interesting SNPs with z -scores with absolute value greater than 4 for the first two components of 60 climatic variables.

Annotation	Gene Ontology	$-\log_{10}(P\text{-value})$
Thylakoid luminal 19 kda chloroplast	Oxygen evolving complex; Photosystem II	9.87
Pentatricopeptide repeat protein	Oxidative stress; Salt stress	8.44
Conserved hypothetical protein	Ubiquitin-specific protease	8.28
Chalcone synthase	Flavonoid biosynthesis; Wound response; Oxidative stress	7.80
Heat shock	Temperature stress	7.67
Dirigent protein pdir18	A Disease response	6.56
Heat shock transcription factor hsf5	Regulation of transcription; Response to stress	6.15
Zinc finger	Transcription; DNA binding; Zinc ion binding	5.84
Probable n-acetyltransferase hookless 1	Auxin signaling; Photomorphogenesis; Ethylene response	5.78
Calcium-binding pollen allergen	Polcalcin; Calcium ion binding	4.61
Geranylgeranyl diphosphate synthase	Cholesterol Biosynthesis; Isoprenoid biosynthesis	4.59
Hypothetical protein OsI_04393	Trehalose-6-phosphate phosphatase	4.59
Potassium proton antiporter	Potassium ion transport; Solute:hydrogen antiporter	5.54
DNA mismatch repair	DNA repair; Regulation of DNA recombination	5.44

TABLE S1: Loblolly pines. SNP identifier and annotation for SNPs with z -scores with absolute value greater than 4 for the first two components of 60 climatic variables.

SNP	Annotation	$-\log_{10}(\text{P-value})$
2-4107-01-438	thylakoid lumenal 19 kda chloroplast	9.87
0-10719-01-95	pentatricopeptide repeat protein	8.44
2-1087-01-86	conserved hypothetical protein [Ricinus communis]	8.28
2-1818-01-168	chalcone synthase	7.80
CL17Contig1-03-443	heat shock	7.67
0-9449-02-292	dirigent protein pdir18	6.56
0-18317-01-495	potassium proton antiporter	6.46
UMN-CL194Contig1-04-130	dna mismatch repair	6.24
0-17238-01-294	Nodulin MtN21 family protein	6.20
0-17776-01-96	heat shock transcription factor hsf5	6.15
0-8823-01-306	squamosa promoter-binding	5.91
2-4856-01-162	zinc finger	5.84
0-4838-01-307	probable n-acetyltransferase hookless 1	5.78
2-3236-01-225	arabinogalactan-like protein	5.76
0-768-02-400	protein kinase family protein	5.72
UMN-5299-01-201	importin-alpha re-	5.33
2-4724-01-136	protein kinase	4.98
0-18887-02-633	amino acid transporter	4.94
CL996Contig1-03-68	af448201 1 alpha-xylosidase	4.93
2-3884-02-413	sf21d1 splice variant protein	4.92
UMN-CL148Contig1-02-220	Histone 2	4.82
CL3851Contig1-05-68	proliferating cell nuclear antigen	4.81
CL2121Contig1-05-658	glycolipid transfer	4.74
CL763Contig1-06-141	calcium-binding pollen Polcalcin	4.61
0-16664-01-58	geranylgeranyl diphosphate synthase	4.59
UMN-1598-02-647	hypothetical protein OsI 04393 [Oryza sativa Indica Group]	4.59
2-7619-01-193	target of myb1	4.57
2-2125-01-274	modulation receptor kinase	4.40
CL3162Contig1-02-257	small gtp-binding protein	4.32
0-13722-01-343	dirigent-like protein	4.22
0-8922-01-655	TIFY domain containing protein	6.01
0-18317-01-495	potassium proton antiporter	5.54
UMN-CL194Contig1-04-130	dna mismatch repair	5.44
CL1381Contig1-01-188	aintegumenta-like protein	5.26
CL3851Contig1-05-68	proliferating cell nuclear antigen	4.52
2-2125-01-274	modulation receptor kinase	4.27

TABLE S2: Climatic variables used in the analysis of the HGDp data set.

BIO1	Annual Mean Temperature
BIO2	Mean Diurnal Range (Mean of monthly (max - min)
BIO3	Isothermality (BIO2/BIO7)
BIO4	Temperature Seasonality (standard deviation * 100)
BIO5	Max Temperature of Warmest Month
BIO6	Min Temperature of Coldest Month
BIO7	Temperature Annual Range (BIO5-BIO6)
BIO8	Mean Temperature of Wettest Quarter
BIO9	Mean Temperature of Driest Quarter
BIO10	Mean Temperature of Warmest Quarter
BIO11	Mean Temperature of Coldest Quarter

TABLE S3: Human data. HGDp SNPs with z -scores with absolute value greater than 7 in genes with molecular (Mol), and biological (Bio) functions associated with these genes.

SNP	CHR	BP	Gene	$-z$ -score	Gene function
7529482	1	203659355	ATP2B4/intron	7.15	(Mol) calmodulin binding; protein binding; hydrolase activity; calcium-transporting ATPase activity; metal ion binding; nucleotide binding; ATP binding; hydrolase activity, acting on acid anhydrides, catalyzing transmembrane movement of substances; PDZ domain binding (Bio) platelet activation; transport; ATP biosynthetic process; blood coagulation; transmembrane transport; cation transport
3816186	2	42936547	MTA3/nearGene-3	7.35	(Mol) zinc ion binding; sequence-specific DNA binding; metal ion binding; transcription factor activity
4681618	3	150146026	TSC2D2/intron	7.25	(Mol) transcription factor activity
9784335	3	150159767	TSC2D2/intron	7.21	(Bio) response to osmotic stress
10935800	3	150149696	TSC2D2/intron	7.36	
11708779	3	55934939	ERC2/intron	7.40	(Mol) protein binding
144173	7	100416250	EPHB4/cds-synon	8.90	(Mol) protein binding; protein-tyrosine kinase activity; ephrin receptor activity; nucleotide binding; transmembrane receptor protein tyrosine kinase activity; receptor activity; ATP binding
					heart morphogenesis; cell migration during sprouting angiogenesis; protein amino acid autophosphorylation; multicellular organismal development; ephrin receptor signaling pathway; angiogenesis; cell adhesion
3807496	7	16821355	TSPAN13/intron	7.46	—
4729616	7	100462565	SLC12A9/intron	7.35	(Mol) cation:chloride symporter activity
					(Bio) transmembrane transport
6942733	7	100350763	ZAN/missense	7.41	(Bio) cell-cell adhesion; binding of sperm to zona pellucida
10953303	7	100365613	ZAN/missense	7.37	
989465	8	32105334	NRG1/intron	7.04	(Mol) protein binding; transmembrane receptor protein tyrosine kinase activator activity; growth factor activity; ErbB-3 class receptor binding; cytokine activity; transcription cofactor activity; protein tyrosine kinase activator activity; receptor tyrosine kinase binding; receptor binding
10096233	8	32115256	NRG1/intron	7.15	(Bio) nervous system development; regulation of protein heterodimerization activity; Notch signaling pathway; positive regulation of cell adhesion; transmembrane receptor protein tyrosine kinase activation (dimerization); neural crest cell development; cellular protein complex disassembly; wound healing; regulation of protein homodimerization activity; ventricular cardiac muscle cell differentiation; positive regulation of striated muscle cell differentiation; positive regulation of cell growth; cardiac muscle cell differentiation; cell proliferation; embryonic development; mammary gland development; anti-apoptosis; cell communication; negative regulation of secretion; negative regulation of transcription, DNA-dependent; transmembrane receptor protein tyrosine kinase signaling pathway; positive regulation of cardiac muscle cell proliferation
10756461	9	13185149	MPDZ/intron	7.79	(Mol) protein C-terminus binding; protein binding
					(Bio) interspecies interaction between organisms
1538677	10	72543579	C10orf27/intron	8.11	(Bio) multicellular organismal development; spermatogenesis; cell differentiation
12415051	10	72543913	C10orf27/intron	8.36	
10998340	10	70383593	TET1/intron	8.24	(Mol) oxidoreductase activity, acting on single donors with incorporation of molecular oxygen, incorporation of two atoms of oxygen; structure-specific DNA binding; zinc ion binding; iron ion binding; metal ion binding; oxidoreductase activity
					(Bio) inner cell mass cell differentiation; regulation of transcription, DNA-dependent; stem cell maintenance; chromatin modification

TABLE S3: (bis)

SNP	CHR	BP	Gene	$-z$ -score	Gene function
2403221	11	9852475	SBF2/intron	8.33	(Mol) protein binding; protein homodimerization activity; phosphatase regulator activity; phosphoinositide binding; phosphatase binding (Bio) myelination; protein tetramerization
4910295	11	11311743	GALNTL4/intron	7.27	(Mol) transferase activity; transferring glycosyl groups; polypeptide N-acetylgalactosaminyltransferase activity; sugar binding
11066776	12	114264827	RBM19/intron	7.04	(Mol) RNA binding; nucleotide binding
9543476	13	74425228	KLF12/intron	7.16	(Bio) positive regulation of embryonic development; multicellular organismal development (Mol) DNA binding; zinc ion binding; metal ion binding; transcription corepressor activity; transcription factor activity
1760907	14	20844859	TEP1/intron	7.15	(Bio) regulation of transcription from RNA polymerase II promoter; positive regulation of transcription from RNA polymerase II promoter
6063071	20	45737763	EYA2/intron	7.09	(Mol) telomerase activity; RNA binding; nucleotide binding; ATP binding (Bio) telomere maintenance via recombination (Mol) protein binding; hydrolase activity; magnesium ion binding; protein tyrosine phosphatase activity
2294352	22	40827319	MKL1/intron	7.96	(Bio) istone dephosphorylation; striated muscle development; regulation of transcription, DNA-dependent; apoptosis; multicellular organismal development; mesodermal cell fate specification; chromatin modification; DNA repair
3827382	22	40881403	MKL1/intron	7.73	(Mol) actin monomer binding; leucine zipper domain binding; protein binding; nucleic acid binding; transcription coactivator activity
6001912	22	40828361	MKL1/intron	7.26	(Bio) positive regulation of transcription, DNA-dependent; anti-apoptosis; smooth muscle cell differentiation; positive regulation of transcription from RNA polymerase II promoter
6001913	22	40836753	MKL1/intron	7.51	
17002034	22	40996367	MKL1/intron	8.01	
5917471	X	37652518	CYBB/intron	7.04	(Mol) protein binding; FAD binding; electron carrier activity; protein heterodimerization activity; metal ion binding; superoxide-generating NADPH oxidase activity; heme binding; voltage-gated ion channel activity; oxidoreductase activity
5944708	X	25000842	POLA1/intron	7.63	(Bio) respiratory burst; superoxide metabolic process; innate immune response; ion transport; inflammatory response; superoxide release; hydrogen peroxide biosynthetic process (Mol) DNA primase activity; metal ion binding; nucleotide binding; DNA-directed DNA polymerase activity; nucleotidyltransferase activity; transferase activity; protein binding; DNA binding; protein heterodimerization activity; purine nucleotide binding; double-stranded DNA binding; nucleoside binding; chromatin binding; pyrimidine nucleotide binding (Bio) DNA replication initiation; M/G1 transition of mitotic cell cycle; interspecies interaction between organisms; DNA replication, synthesis of RNA primer; DNA strand elongation during DNA replication; leading strand elongation; DNA repair; lagging strand elongation; double-strand break repair via nonhomologous end joining; telomere maintenance via semi-conservative replication; G1/S-specific transcription in mitotic cell cycle; cell proliferation; DNA synthesis during DNA repair; telomere maintenance via recombination; nucleobase, nucleoside, nucleotide and nucleic acid metabolic process; mitotic cell cycle; DNA replication checkpoint; S phase of mitotic cell cycle; DNA replication; telomere maintenance; G1/S transition of mitotic cell cycle
6643647	X	153086372	PDZD4/intron	7.95	—

Gibbs Sampling algorithm for the LFMM

5.1 Prior Distribution

Let D is the number of environmental variables. $I_{i,\ell}$ is the indicator variable equal to 0 if the data are missing and 1 otherwise. $N(\mu, \Sigma)$ is the normal distribution of mean μ and of covariance matrix Σ . $\Gamma^{-1}(a, b)$ is the inverse-gamma distribution of shape a and of rate b (ie of scale $\frac{1}{b}$).

The prior distributions on the LFMM parameters are given by:

$$\text{for all } i, \ell \quad G_{i,\ell} | U_i, V_\ell, \beta_\ell, \mu_\ell, \sigma^2 \sim N(X_i \beta_\ell + \mu_\ell + U_i^T V_\ell, \sigma^2)^{I_{i,\ell}} \quad (10)$$

$$\text{for all } i \quad U_i | \sigma_U^2 \sim N(0, \sigma_U^2 I_K) \quad (11)$$

$$\text{for all } \ell \quad V_\ell | \sigma_V^2 \sim N(0, \sigma_V^2 I_K) \quad (12)$$

$$\text{for all } \ell, d \quad \beta_{d,\ell} | \sigma_{\beta(d)}^2 \sim N(0, \sigma_{\beta(d)}^2) \quad (13)$$

$$\text{for all } \ell \quad \mu_\ell | \sigma_\mu^2 \sim N(0, \sigma_\mu^2) \quad (14)$$

$\sigma_V^2 = 1$ and σ^2 is updated at each iteration by the current residual variance.

for all d $\sigma_{\beta(d)}^2$, σ_μ^2 and σ_U^2 follow an inverse-gamma distribution $\Gamma^{-1}(\eta, \eta)$ where $\eta = 10^3$.

5.2 Conditional Distribution

The LFM Model is a hierarchical model which conditional distributions can be described as follows:

$$p(\sigma_U^2 | U, \eta) = \Gamma^{-1}(\eta + \frac{NK}{2}, \frac{1}{2} \sum_i U_i^T U_i + \eta) \quad (15)$$

$$p(\sigma_{\beta(d)}^2 | \beta, \eta) = \Gamma^{-1}(\eta + \frac{M}{2}, \frac{1}{2} \sum_l \beta_{d,\ell}^2 + \eta) \quad (16)$$

$$p(\sigma_\mu^2 | \mu, \eta) = \Gamma^{-1}(\eta + \frac{M}{2}, \frac{1}{2} \sum_\ell \mu_\ell^2 + \eta) \quad (17)$$

$$p(U_i | G, V, \beta, \mu, \sigma_U^2, \sigma^2) = N(\mu_U^i, \Delta_U^{i-1}) \quad (18)$$

where

$$\Delta_U^i = \sigma_U^{2-1} I_K + \sigma^{2-1} \sum_\ell V_\ell V_\ell^T \text{ and } \mu_U^i = \sigma^{2-1} (\Delta_U^i)^{-1} \sum_\ell (G_{i,\ell} - X_i \beta_\ell - \mu_\ell) V_\ell \quad (19)$$

$$p(V_\ell | G, U, \beta, \mu, \alpha_G) = N(\mu_V^\ell, \Delta_V^{\ell-1}) \quad (20)$$

where

$$\Delta_V^\ell = \sigma_V^{2-1} I_K + \sigma^{2-1} \sum_i U_i U_i^T \text{ and } \mu_V^\ell = \sigma^{2-1} (\Delta_V^\ell)^{-1} \sum_i (G_{i,\ell} - X_i \beta_\ell - \mu_\ell) U_i \quad (21)$$

$$p(\beta_\ell | G, U, V, \mu, \sigma_\beta(1)^2, \dots, \sigma_\beta(d)^2, \sigma^2) = N(\mu_\beta^\ell, \Delta_\beta^{\ell-1}) \quad (22)$$

where

$$\Delta_\beta^\ell = \text{diag}(\sigma_\beta(1)^{2-1}, \dots, \sigma_\beta(d)^{2-1}) + \sigma^{2-1} \sum_i X_i^T X_i \text{ and } \mu_\beta^\ell = \sigma^{2-1} (\Delta_\beta^\ell)^{-1} \sum_i (G_{i,\ell} - U_i^T V_\ell - \mu_\ell) X_i^T \quad (23)$$

$$p(\mu_\ell | G, U, V, \beta, \sigma_\mu^2, \sigma^2) = N(\mu_\mu^\ell, \Delta_\mu^{\ell-1}) \quad (24)$$

where

$$\Delta_\mu^\ell = \sigma_\mu^{2-1} + \sigma^{2-1} N \text{ and } \mu_\mu^\ell = \sigma^{2-1} (\Delta_\mu^\ell)^{-1} \sum_i (G_{i,\ell} - U_i^T V_\ell - X_i \beta_\ell) \quad (25)$$

5.3 Main algorithm

$nIter$ is the number of iterations and $burn$ is the number of iterations for burning.

1. Initialize model parameters

$$U = 0_{K,N}$$

$$V = 0_{K,M}$$

$$\beta = 0_{M,D}$$

$$\mu = 0_{M,1}$$

2. For $n = 1 \dots nIter$

- input missing values at locus ℓ for individu i ,

$$G_{i,\ell} \leftarrow U_i^{(n-1)T} V_\ell^{(n-1)} + X_i^{(n-1)} \beta_\ell^{(n-1)}$$

- update the residual variance

$$\sigma^{2(n)} = \text{var}(G - U^{(n-1)T} V^{(n-1)} - X^{(n-1)} \beta^{(n-1)})$$

- sample the hyperparameters

$$\sigma_U^{2(n)} \sim p(\sigma_U^2 | U^{(n-1)}, \eta)$$

$$\sigma_\beta^{2(n)} \sim p(\sigma_\beta^2 | \beta^{(n-1)}, \eta)$$

$$\sigma_\mu^{2(n)} \sim p(\sigma_\mu^2 | \mu^{(n-1)}, \eta)$$

- for each locus ℓ , sample

$$\mu_\ell^{(n)} \sim p(\mu_\ell | U^{(n-1)}, V^{(n-1)}, \beta^{(n-1)}, \sigma_\mu^{2(n)}, \sigma^{2(n)})$$

$$\beta_\ell^{(n)} \sim p(\beta_\ell | U^{(n-1)}, V^{(n-1)}, \mu^{(n)}, \sigma_\beta(1)^{2(n)}, \dots, \sigma_\beta(d)^{2(n)}, \sigma^{2(n)})$$

- for each individu i , sample

$$U_i^{(n)} \sim p(U_i | \mu^{(n)}, V^{(n-1)}, \beta^{(n)}, \sigma_U^{2(n)}, \sigma^{2(n)})$$

- for each locus l , sample

$$V_\ell^{(n)} \sim p(V_\ell | \mu^{(n)}, U^{(n)}, \beta^{(n)}, \sigma^{2(n)})$$

3. compute the parameters

$$U = \text{mean}(U^{(burn+1)}, \dots, U^{(nIter)})$$

$$V = \text{mean}(V^{(burn+1)}, \dots, V^{(nIter)})$$

$$\beta = \text{mean}(\beta^{(burn+1)}, \dots, \beta^{(nIter)})$$

$$\mu = \text{mean}(\mu^{(burn+1)}, \dots, \mu^{(nIter)})$$

$$Z = \text{mean}(\beta^{(burn+1)}, \dots, \beta^{(nIter)}) / \text{var}(\beta^{(burn+1)}, \dots, \beta^{(nIter)})^{\frac{1}{2}}$$